



Mass flow and heat transfer characteristics of lift tube technology

Michael Jacobson*, Cedric Briens, Franco Berruti

Institute for Chemicals and Fuels from Alternative Resources, Department of Chemical and Biochemical Engineering, The University of Western Ontario, London, ON, Canada N6A 5B9

ARTICLE INFO

Article history:

Received 8 February 2008

Received in revised form 16 July 2008

Accepted 28 July 2008

Keywords:

Fluidized bed
Vertical transport
Motive nozzle
Lift tube
Heat transfer

ABSTRACT

An innovative vertical transport tube system has been developed to enhance heat transfer between fluidized beds and axial solids circulation within a fluidized bed reactor. Vertical lift tubes pick up particles from the bottom of the reactor, carry them through a fluidized bed burner before discharging them above the reactor bed surface. A full-scale experimental setup was designed to test the effects of different operating conditions on the solids flow through the lift tube. The heat transfer and mass flowrate through the lift tube are altered by varying the fluidization conditions, the motive gas flowrate and the location of a motive gas nozzle with respect to the tube. Increasing the pressure downstream of the lift tube reduces the solids flow. A preliminary study on the heat transfer benefit of the lift tubes was also performed on another laboratory apparatus: implementation of a single lift tube increased the heat transfer coefficient between the central and annular bed from 25 to 400 W/m² K at optimal flow conditions. This technology has been successfully implemented in a full-scale annular pyrolysis reactor.

© 2008 Elsevier B.V. All rights reserved.

1. Introduction

In many processes, the use of fluidized bed reactors is limited by the inability to transfer enough heat in or out of the bed. Many situations also require two fluidized beds to be completely segregated to avoid contamination or reaction between the compounds present. A new technology has, therefore, been developed to enhance heat transfer in standard and annular fluidized bed reactors. In the case of an endothermic reaction, vertical lift tubes pick up particles from the fluidized bed reactor, carry them through a high temperature burner, and then discharge them above the reactor bed surface. In case of exothermic reactions, solids can be transported through the lift tube and through a cooling water bath for heat removal. A diagram of these scenarios is shown in Fig. 1. As a result of the vertical movement of the solids, the lift tubes also provide axial solids mixing. This paper focuses on the identification of the operating conditions required to maximize the solids flow through the lift tubes, as pneumatic transport line studies have found the heat transfer to be positively correlated to the solids flow [1,2]. Results of a preliminary heat transfer experiment will also be presented.

Although there is no published study of similar lift tubes, many researchers have investigated the effects of tube position and fluidization velocity on the flow of solids through a draft tube in a

fluidized bed [3–7]. Song et al. [6] found that the type of distributor had little effect on the solids flow, as long as the fluidization gas was introduced in a way that allowed for gas bypassing from the annulus to the draft tube. Song's experimental setup was similar to that used in this study, the distance between the tube and distributor was variable and a separate sparger plate controlled the gas flow to the draft tube. These authors found that the flowrate of solids increased with increasing annulus fluidization gas, tube gas, and gap height between the tube and the gas injector at higher annulus gas flowrates.

Yang and Keairns [7], however, showed that in a spout-fluid bed with draft tube, larger gap heights resulted in a decrease in the solids flowrate. They attributed this to startup problems created by the tube gas bypassing the draft tube. Therefore, in a fluidized bed with a draft tube, at some critical gap distance, gas bypassing will switch direction from annulus-to-tube to tube-to-annulus; this causes a change in the dynamics of the system which results in a decrease of the solids flowrate. Muir et al. [8] found, in a spout-fluid bed, that this critical length was directly related to the diameter of the motive gas jet at the inlet of the draft tube. When the diameter of the jet was equal to the diameter of the draft tube, maximum solids flow was achieved. With increased nozzle gas flow, the diameter of the jet expanded, and a reduction in the solids flow was observed. Visual observations attributed this to the bypassing of nozzle gas to the annular bed and a reduction in the ability for particle clusters (slugs) to form.

Hulet et al. [9] used a vertical tube immersed in a fluidized bed to transport solids out of the bed. The geometry of the nozzle and of the draft tube inlet had a large impact on the solids flowrate

* Corresponding author at: Faculty of Engineering, The University of Western Ontario, London, ON, Canada N6A 5B9. Tel.: +1 519 350 3852; fax: +1 519 661 3498.
E-mail address: mjacobso2@uwo.ca (M. Jacobson).

Nomenclature

d_{p50}	particle Sauter mean diameter (μm)
D_{bed}	bed inner diameter (m)
D_T	lift tube inner diameter (mm)
DAQ	data acquisition
F_V	fluidization velocity (mm/s)
H_i	immersion depth of lift tube (m)
H_{gap}	distance between the exit of the motive nozzle and the lift tube entrance (mm)
H_F	heated bed/combustor simulator fluidization velocity (mm/s)
ρ_s	particle density (kg/m^3)
T_D	motive nozzle throat diameter (mm)

entrained into the tube. They were able to greatly increase the entrained solids flow by adding appropriate internals [9,10].

Zhang et al. [4] used a three-phase fluidized bed coater with a liquid nozzle placed below the entrance to a draft tube. A constriction between the draft tube and the wall of the annulus was found to cause a decrease in the flow. This was tested with a conical bed by adjusting the location of the draft tube so that the space between the conical wall and the tube entrance could be reduced. A decrease in this space of only 5 mm reduced the maximum solids flow through the tube by about a third. In order to prevent such a situation from occurring in this study, the lift tube inlet had 10 cm free of obstruction, other than the motive nozzle, in all directions.

2. Experimental setups and method

Experiments were conducted to test the effect of lift tube characteristics and operating conditions on the entrained solids flow,

using the apparatus shown in Fig. 2. The apparatus had an ID of 0.279 m and had an expanded section in order to reduce the loss of entrained solids. The axis of the vertical lift tube was 0.04 m from the wall. The lift tube was 0.616 m long with an ID of 25.4 mm, unless otherwise stated. A horizontal section, 0.1 m in length, connected the lift tube to a cyclone with filter paper at its gas exit, the “funclone”. The solids collected by the funclone flowed down a 51 mm ID tube into a receiving vessel, to be weighed upon completion of an experiment. A 6.35 mm OD motive nozzle with a 2.4 mm ID tip diameter was used to transport the particles, unless otherwise stated. The nozzle was positioned so that the jet would be centered in the lift tube and was secured in this position. Silica sand particles ($d_{p,50} = 200 \mu\text{m}$, $\rho_s = 2650 \text{ kg}/\text{m}^3$) were filled to a slumped bed immersion depth of 0.325 m, unless otherwise stated. A National Instruments USB-6009 data acquisition (DAQ) device recorded the pressure difference between the bed and the receiving vessel.

For each experiment, the bed was fluidized and allowed to reach equilibrium. The DAQ, transport gas flow and a stopwatch were started simultaneously; the transport gas was turned on and off by use of a ball valve. Each experiment was 90 s long, in order to minimize the effects of the reduction of bed height associated with the solids flow into the lift tube, while still providing sufficient time to reduce startup effects on the results. The solids were then weighed and returned to the bed. The conditions studied included: motive nozzle gas flowrate, fluidization velocity, tube immersion depth, lift tube diameter, and the properties of the motive gas used.

A series of experiments was also performed to determine the effects of the pressure at the exit of the lift tube on the solids flowrate through the lift tube. In order to perform these experiments, the pressure in the receiving vessel was increased by the introducing pressurized gas. This artificially increased the pressure to simulate what would happen if a problem occurred downstream of the lift tube.

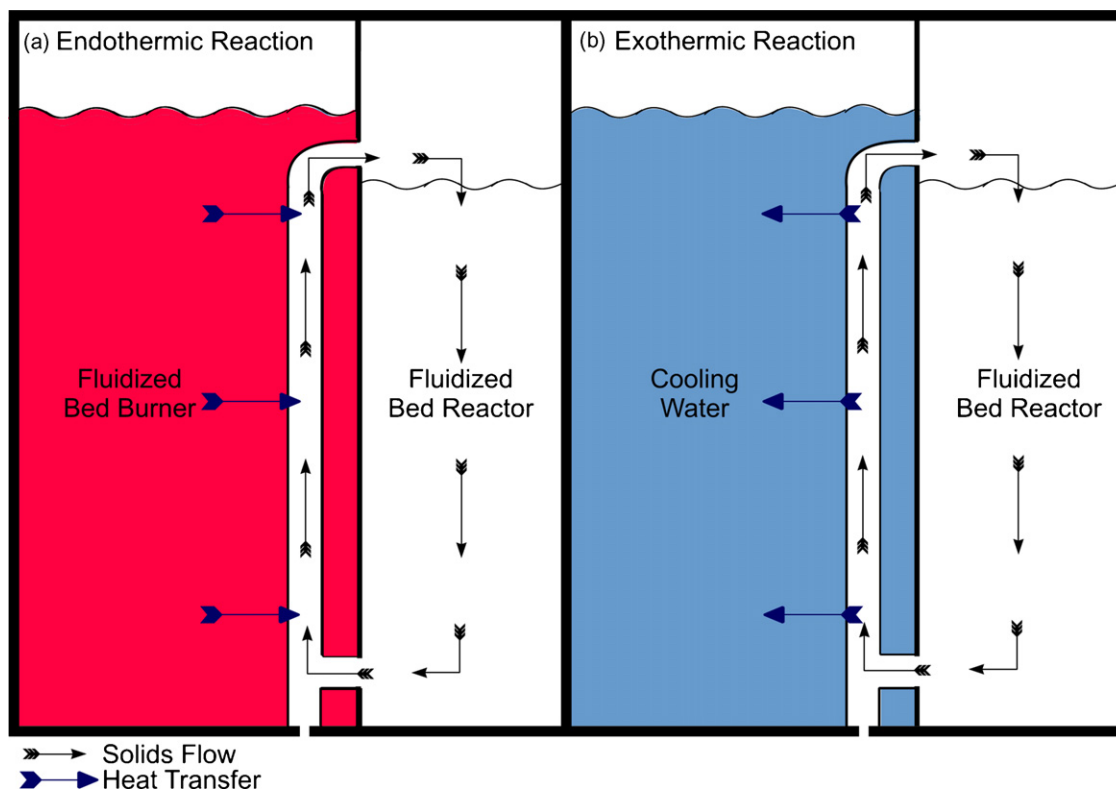


Fig. 1. Lift tube use: (a) endothermic reaction; (b) exothermic reaction.

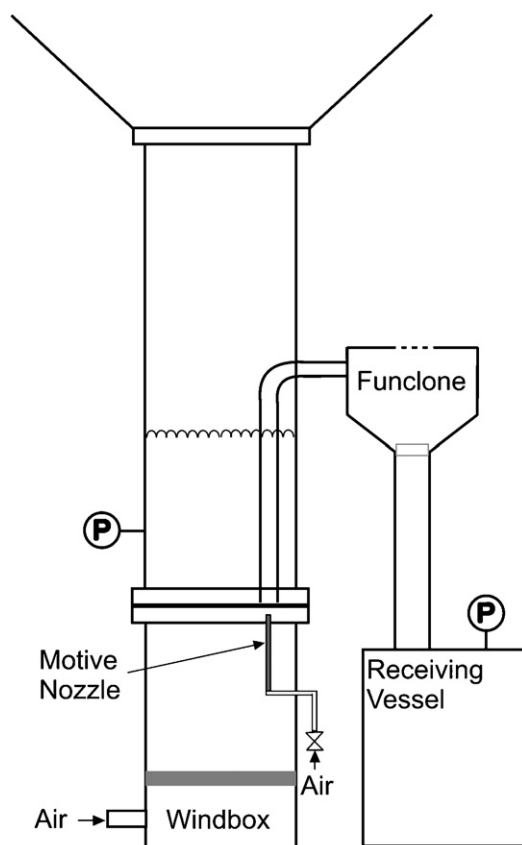


Fig. 2. Mass flow experimental apparatus.

Steady state heat transfer experiments were performed in a separate apparatus shown in Fig. 3. The central bed (1) was heated by two cartridge heaters (2) controlled by an on/off controller to maintain a temperature of 55 °C. Solids were circulated from the bottom of the annular bed (3) through the lift tube (4) immersed in the central bed and back to the top of the annular bed. Motive gas (5) was used to provide the driving force for the solids circulation. The lift tube and silica sand particles used in this apparatus were the same as those used in the previous setup. A fluidized immersion depth of 0.432 m was maintained throughout the experiments.

3. Results and discussion

3.1. Effect of motive gas flowrate

Increasing the motive gas flowrate initially increased the flow of solids through the lift tube. However, as the motive gas flowrate continued to increase, the solid flowrate reached a maximum and then began to decrease, as shown in Fig. 4. A similar trend was also reported in the literature on spouted beds [3,5,6].

This second order trend is a result of a shift in the pressure drop over the length of the lift tube from static holdup dominance to wall friction dominance. As the gas flowrate increases, the pressure drop associated with wall friction increases, as shown in Fig. 5 from a study that used different solids. This increase creates a net decrease in the total pressure available for the solids, thus reducing the amount of solids that can be transported. At low gas flowrates, the static pressure drop associated with the solids dominates causes a flow restriction; as the gas flowrate increases, this pressure drop is reduced by the increase in voidage created within the tube.

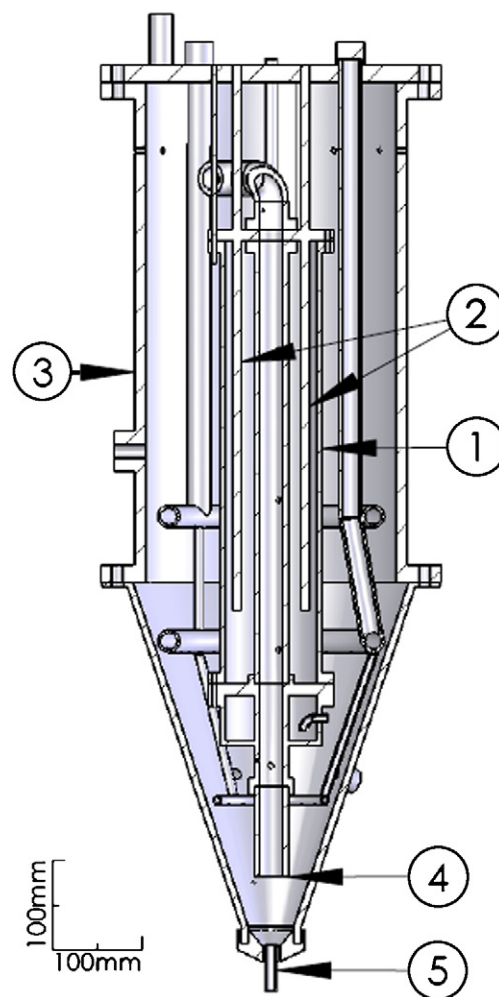


Fig. 3. Heat transfer experimental apparatus.

3.2. Effect of nozzle throat diameter

The maximum solid flowrate was much greater with the 2.6 mm nozzle, as shown in Fig. 6. However, the 1.2 mm nozzle was more efficient since it could transport more solids per kilogram of motive gas, as seen in Fig. 7. This effect is due to the vacuum or ejector

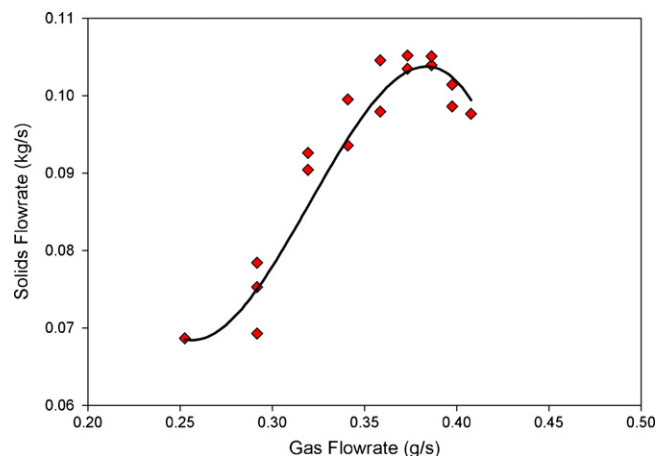


Fig. 4. Effect of gas flowrate on solid flowrate ($T_D = 1.2$ mm, $F_V = 49$ mm/s, $H_{gap} = 15.9$ mm, $D_T = 25.6$ mm, air, $H_i = 0.356$ m).

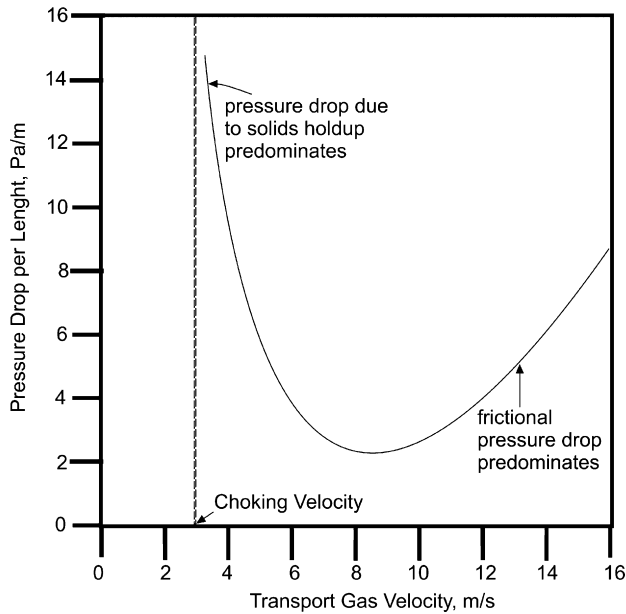


Fig. 5. Dominating pressure drop with increasing gas velocity (adapted from [11]).

effect of the high velocity gas jet issuing from the motive gas nozzle. A smaller nozzle can provide a high momentum at a lower gas flowrate; since there is less motive gas going up the lift tube, there is more room for the fluidization gas to be pulled into the lift tube, bringing solids with it. In addition, a decrease in the pressure drop associated with gas flow is observed when using the smaller nozzle, resulting in an increase in the solids flow.

3.3. Effect of fluidization quality

The velocity of the fluidization gas was increased from 49 to 70 mm/s (the minimum fluidization velocity was 36 mm/s). The increase in fluidization velocity promoted an overall increase in the solids flowrate through the lift tube, as displayed in Fig. 8. The maximum solids flowrate increased because of bed expansion at the higher velocity. This resulted in a larger mass of solids above the lift tube inlet, and hence a higher pressure at the tube inlet, driving more solids into the lift tube. Other studies have shown that the impact of the fluidization gas velocity on the entrained solids flow depends on the system geometry [8,9].

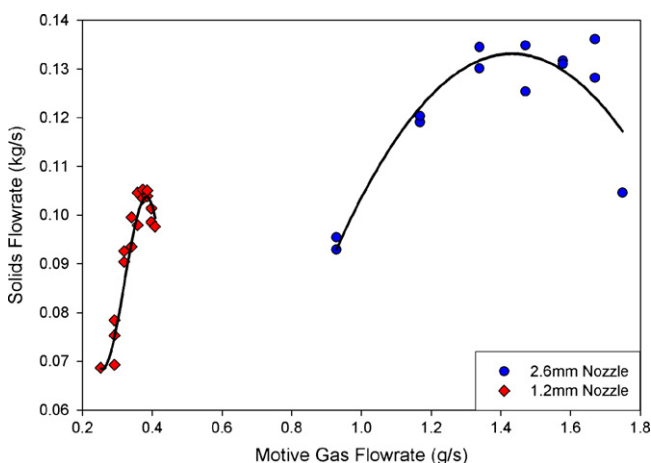


Fig. 6. Effect of nozzle throat diameter on the solid flowrate ($F_V = 49$ mm/s, $H_{\text{gap}} = 15.9$ mm, $D_T = 24.6$ mm, air).

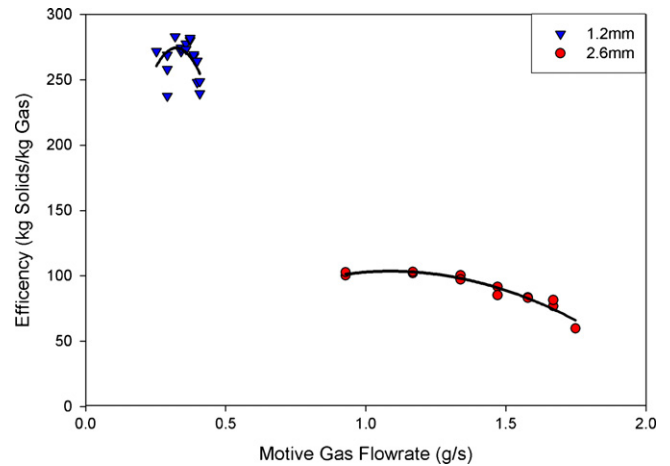


Fig. 7. Gas efficiency for different nozzle diameters ($F_V = 49$ mm/s, $H_{\text{gap}} = 15.9$ mm, $D_T = 24.6$ mm, air, $H_i = 0.356$ m).

3.4. Effect of the immersion depth

The immersion depth of the lift tube had the largest effect on the solid flowrate. Fig. 9 shows that increasing the immersion depth from 0.26 to 0.566 m tripled the maximum solids flowrate. This confirms the beneficial effect of an increased pressure difference between bed and tube exit. By increasing the bed height, a larger bed pressure at the level of the tube inlet provides a stronger driving force; the lift tube pressure drop can then be larger allowing the entrained solids flowrate to be larger. This high flowrate of solids will cause the entrained solids flow to peak at a lower motive gas flowrate. In most situations, this would provide a much more economical process. The lift tubes should be operated with the largest immersion depth possible, therefore the bed height should be just below the outlet of the lift tube for maximum transport of solids if the tube is to discharge solids above the bed surface.

3.5. Effect of lift tube diameter

Varying the diameter of the transport tube while preserving the tube length and geometry helped determine the effect of scale-up. Fig. 10 shows that this scale-up effect is complex. The maximum entrained solids flowrate increases with increasing tube diameter. However, the intermediate tube size of 19.6 mm was the

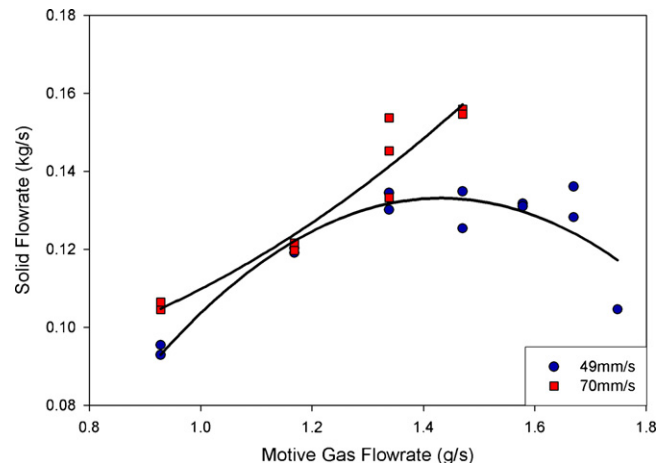


Fig. 8. Effect of fluidization quality on the solid flowrate for a given gas flowrate ($T_D = 2.6$ mm, $H_{\text{gap}} = 25.4$ mm, $D_T = 25.6$ mm, air, $H_i = 0.356$ m).

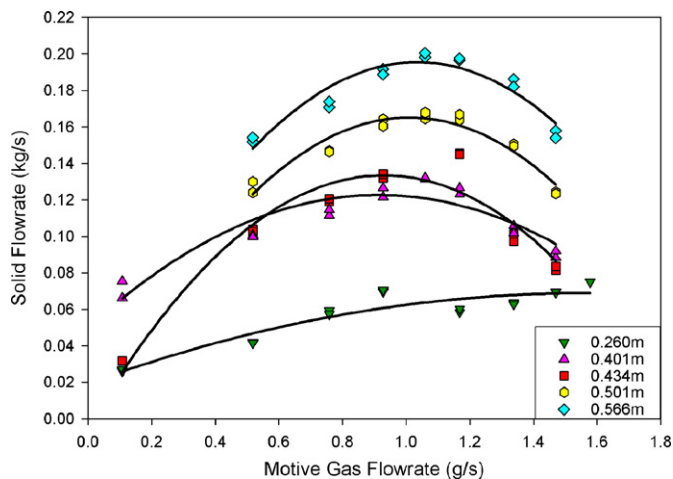


Fig. 9. Effect of immersion depth on the solids flowrate through the lift tube ($T_D = 2.6$ mm, $F_V = 49$ mm/s, $H_{gap} = 9.5$ mm, $D_T = 25.6$ mm, air).

most efficient: more solids were entrained for a given motive gas flowrate.

3.6. Effect of motive gas properties

Different transport gases were used to determine the effects of the molecular mass and the sonic velocity of the motive gas. It can be seen in Fig. 11 that the maximum solids flowrate obtained using the different motive gases was around the same value, 0.12 kg/s. However, as the molecular weight of the motive gas increased so did the mass flowrate of motive gas required for the maximum solids flow. Fig. 12 shows that argon and air have nearly the same optimum molar gas flowrate but that helium transports less solids per mole of gas. The sonic velocity of helium is much larger than the sonic velocity of air but cannot fully compensate for its smaller density; for the same molar flowrate, the kinetic energy of the motive gas is nearly 150% larger for air than helium.

3.7. Gap distance

The effect of the distance between the nozzle tip and the lift tube inlet, H_{gap} , is shown in Fig. 13. At low motive gas flowrates, more solids were entrained from the bed with smaller gaps than for larger gaps, but this trend disappeared at higher motive gas

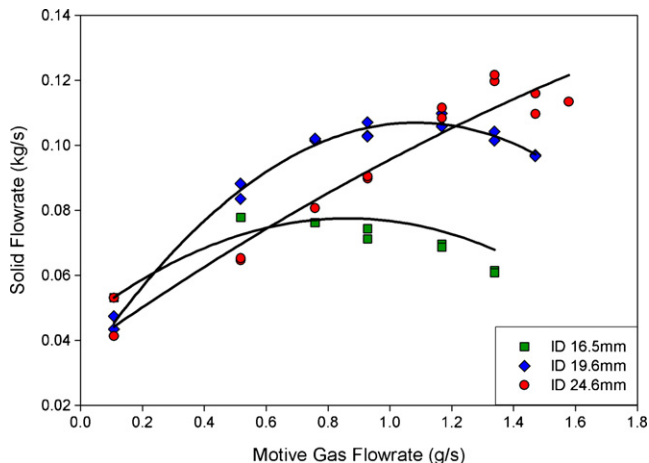


Fig. 10. Effect of the lift tube inner diameter on the flowrate of solids ($T_D = 2.6$ mm, $F_V = 49$ mm/s, $H_{gap} = 25.4$ mm, air, $H_i = 0.356$ m).

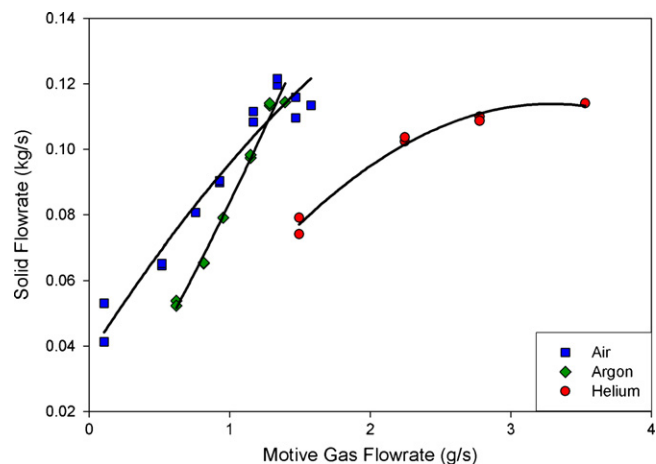


Fig. 11. Effect of motive gas mass flowrate on solid flowrate ($T_D = 2.6$ mm, $F_V = 49$ mm/s, $H_{gap} = 25.4$ mm, $D_T = 25.6$ mm, $H_i = 0.356$ m).

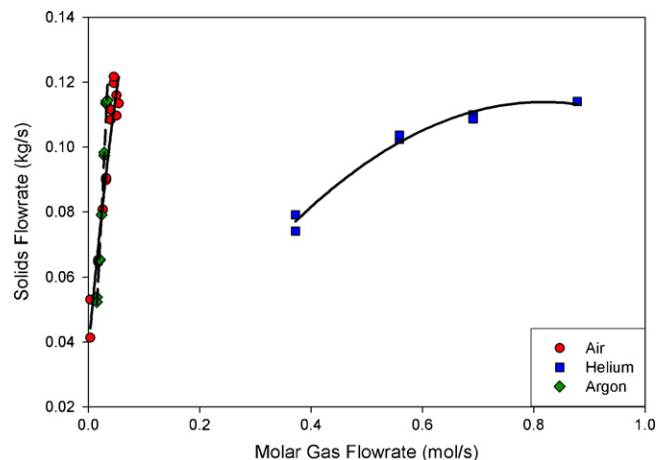


Fig. 12. Effect of motive gas molar flowrate on solid flowrate ($T_D = 2.6$ mm, $F_V = 49$ mm/s, $H_{gap} = 25.4$ mm, $D_T = 25.6$ mm, $H_i = 0.356$ m).

flowrates. At larger gap heights, the width of the motive gas jet at the lift tube level is smaller than the lift tube diameter, resulting in a reduction in solids flow. The diameter of the motive gas jet is reduced as the kinetic energy from the gas flow is transferred to the relatively stationary bed particles at the jet boundary; this decrease

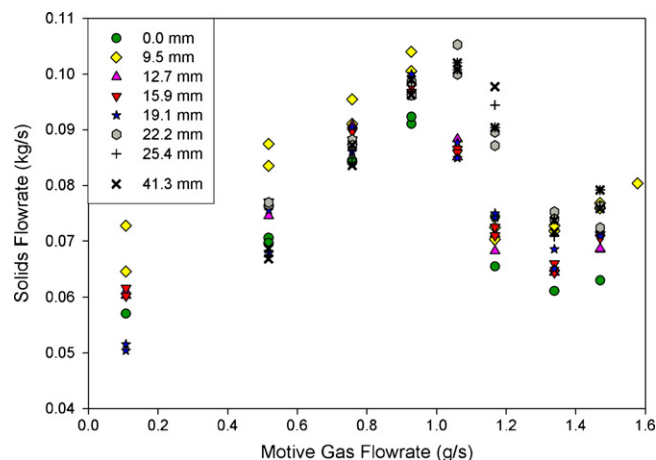


Fig. 13. Effect of the gap distance on the transport of solids through the lift tube ($T_D = 2.6$ mm, $F_V = 49$ mm/s, $D_T = 24.6$ mm, air, $H_i = 0.356$ m).

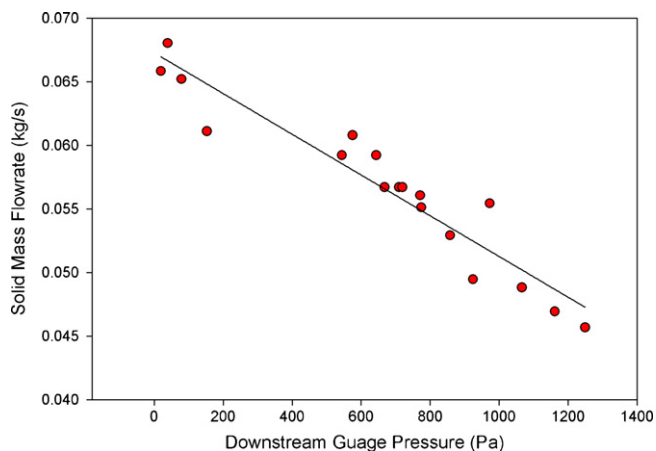


Fig. 14. Effect of downstream pressure on the solids flowrate ($T_D = 2.6$ mm, $F_V = 49$ mm/s, $H_{\text{gap}} = 25.4$ mm, $D_T = 24.6$ mm, air, $H_I = 0.356$ m).

in energy reduces the local stability of the gas jet, resulting in a smaller jet diameter. Larger gap distances create a greater contact area between the bed and the jet, reducing the flow. As the velocity of the motive gas decreases, it is harder for the motive gas to clear the lift tube of solids and form a stable channel.

When the motive gas flowrate is below the optimum value that ensures a jet diameter equal to the inlet diameter, losing some motive gas to the annulus is detrimental to the solids flow, as observed by Muir et al. [8]. On the other hand, when the motive gas flowrate is above its optimum value, for a given gap height, losing some motive gas to the fluidized bed by increasing the gap height is beneficial. This is because, in this case, reducing the motive gas going into the tube reduces the pressure drop inside the tube, reducing the pressure at the tube inlet and increasing the pressure driving force for solids flow into the tube. The bypassing gas also adds to the fluidization quality which also accounts for some of the increase in solids flow. Placing the motive gas tube at the lift tube entrance is never beneficial, as it reduces the area for mass flow.

3.8. Downstream pressure

A set of experiments were performed in order to test for the effects of pressure buildup downstream of the lift tube on the solids flowrate through the lift tube. The physical and operating conditions were kept constant, except for a variance in the gas

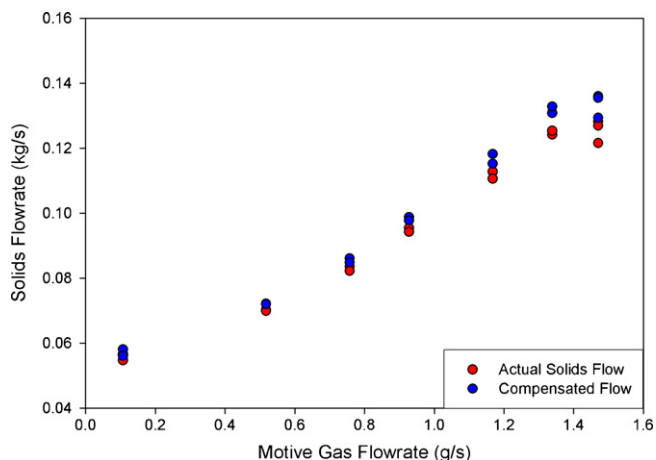


Fig. 15. Compensation for downstream gas buildup ($T_D = 2.6$ mm, $F_V = 49$ mm/s, $H_{\text{gap}} = 25.4$ mm, $D_T = 24.6$ mm, air, $H_I = 0.356$ m).

flow to the receiving vessel. As can be seen in Fig. 14, the downstream pressure appeared to have a large linearly negative effect on the solids flowrate. By increasing the downstream pressure while maintaining the same bed height upstream of the tube, the pressure difference across the tube, which is the driving force for solids flow, decreases.

It was thought that the increase in the nozzle gas flow would reach a point where the funclone was no longer able to handle the flow of gas and thus a pressure buildup would occur downstream of the lift tube. If this was the case, then the peak in the non-monotonic curve shown in Fig. 4 could have been a result of gas buildup. However, when compensating for the pressure drop caused by this flow restriction, it was found that it had a negligible effect, except at high nozzle flowrates, as shown in Fig. 15.

3.9. Global explanation

A simple pressure balance, Equation 1,¹ shows that the maximum flow of solids through the lift tube can be achieved by increasing the immersion depth and minimizing the pressure drops associated with friction (ΔP_f) and solids holdup (ΔP_h) in the tube as well as the pressure at the tube exit. It has been shown that the solids flow variation with gas velocity in the lift tube is the inverse of the variation of the pressure gradient (Fig. 5) and thus maximum solids flow is achieved when the total pressure drop along the tube (ΔP_{tube}) is minimized. This was confirmed when helium was used as the transport gas, and it is believed that it would also have been confirmed with argon if funclone pressure limitations had not prevented higher flows from being tested. Increasing the tube diameter also helps to reduce the frictional pressure drop (ΔP_f), thus allowing more solids to be transported for the same driving force. However, at the same time, the broader diameter decreases the stability of the flow within the lift tube.

$$\Delta P_{\text{inlet}} = P_{\text{exit}} + \Delta P_{\text{tube}} = P_{\text{exit}} + \Delta P_h + \Delta P_f \quad (1)$$

Increasing the immersion depth and fluidization quality increase the driving force for the transport by increasing the pressure in the bed at the inlet of the lift tube. Increasing the bed pressure then increases the pressure drop available to be allocated to solids flow. A pressure increase downstream of the lift tube has a negative effect on the solids flow.

Gas bypassing from the annulus to the lift tube can be beneficial or detrimental to solids flow depending on the other operating conditions. Further increasing of gas flow beyond the optimum value causes an increase in frictional pressure drop (ΔP_f): the solids flow must be reduced to decrease the pressure drop caused by the solids holdup in the lift tube (ΔP_h), since the driving force (ΔP_{inlet}) is the same. Before the optimum value has been reached, the total pressure drop across the lift tube is hindered by slower moving slugs, which increase the solids holdup, resulting in a smaller solids flowrate through the lift tube; increasing the gas bypassing would then help propel these solids through the lift tube faster, thus increasing their flow.

A summary of the effects various parameters have on the pressure balance and stability of lift tube flow, based on Equation 1 and visual observations is given in Table 1.

3.10. Heat transfer boost

The mass flowrate through the lift tube in the simulated heated bed is given in Fig. 16 for various motive gas flowrates. The transition between dense and dilute phase is labeled and was determined

¹ Equation 1: Lift Tube Pressure Balance.

Table 1
Summary of pressure balance trends with increasing various parameters

Parameter increased	ΔP_{inlet}	ΔP_{exit}	ΔP_{h}	ΔP_{f}	Stability
Nozzle flowrate	–	↑	↓	↑	↑
Fluidization quality	↑	–	–	–	↑
Immersion depth	↑	–	–	–	–
Lift tube diameter	–	–	–	–	↓
Nozzle gas molecular weight	–	↑	–	↑	–
Gap distance	–	↓	–	↓	↓
Downstream pressure	–	↑	–	–	–

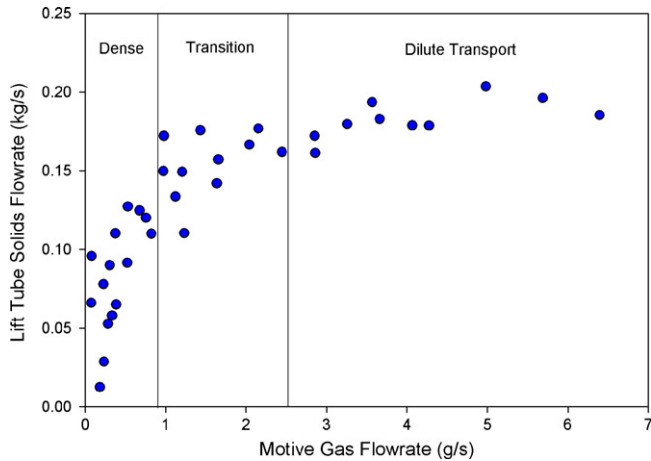


Fig. 16. Solids mass flowrate through the lift tube in heat transfer apparatus ($F_V = 0.18$ m/s, $H_{\text{gap}} = 66.2$ mm, $D_T = 24.6$ mm, air, $H_i = 0.432$ m).

through visual observations. It was found that by using a single lift tube, the overall heat transfer coefficient between the central and annular beds could be increased from 25 to 400 W/m²K, as shown in Fig. 17. The heat transfer coefficient increases linearly as the transition to dilute phase transport is approached and then decreases exponentially as dilute phase flow is developed. Regime detection is therefore critical to the optimal use of these tubes for heat transfer. Further experiments are needed to investigate the effects of operating conditions on the boost in heat transfer provided by the lift tube.

4. Industrial application

Although there are an endless number of applications for this technology, this technology has been successfully implemented in

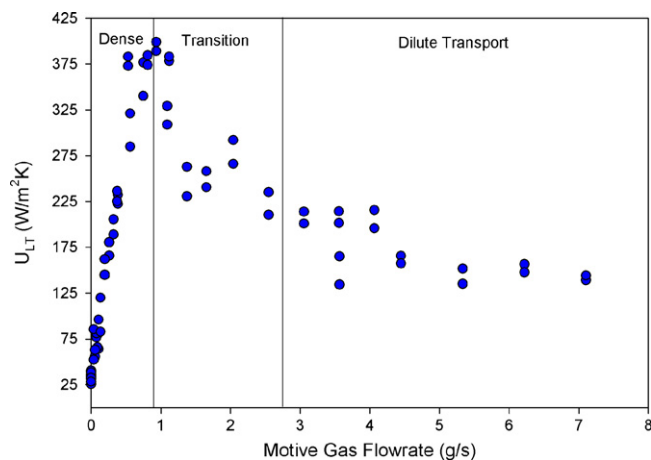


Fig. 17. Effect of motive gas mass flowrate on the overall heat transfer coefficient ($F_V = 0.18$ m/s, $H_{\text{gap}} = 66.2$ mm, $D_T = 24.6$ mm, air, $H_i = 0.432$ m).

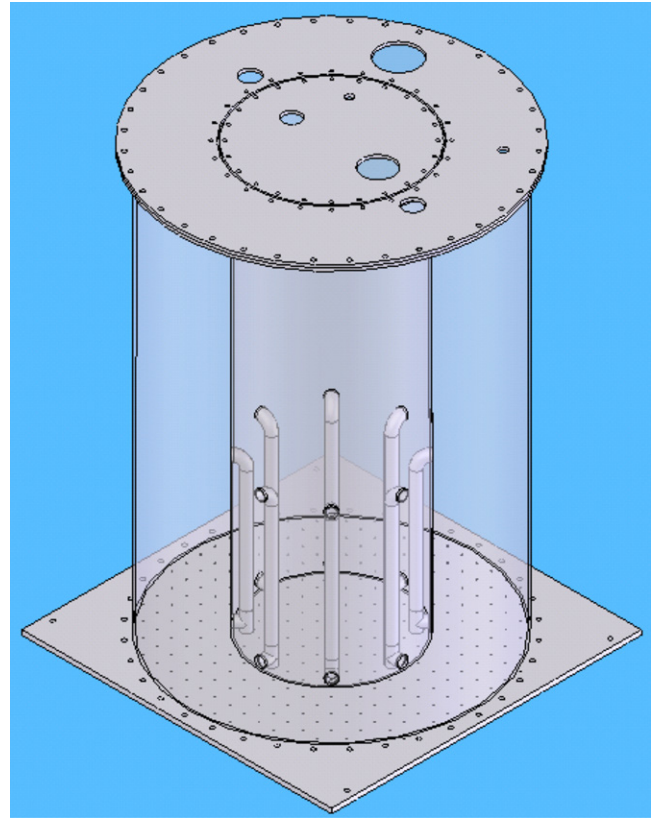


Fig. 18. Agri-Therm mobile pyrolysis reactor.

an annular pyrolysis reactor created by Agri-Therm Ltd, shown in Fig. 18. Fluidized bed pyrolysis uses a hot bed of sand to transfer heat to biomass particles in the absence of oxygen, causing them to thermally crack. As a result, the bed needs constant heat renewal in order to maintain consistent temperature. The sand in the annular reactor can be transported via the lift tubes into a central fluidized bed burner, where heat is generated by combustion of hydrocarbon gases, before being distributed back to the annular reactor. This sand circulation results in a considerable increase in heat transfer. The added benefit of this sand circulation is that the sand deposited on the surface of the bed from the lift tube is able to pull down some of the lighter, unreacted, biomass which tends to float on the surface of the fluidized sand bed, thus enhancing the overall axial mixing of the biomass through the sand bed.

5. Conclusions

Mass flow experiments were performed with the new lift tube technology in order to ensure the proper operating conditions for maximizing the solids flowrate. It was shown that as the gas flowrate increased, a larger nozzle diameter yielded higher solids flow, however a smaller nozzle was more efficient. The immersion depth and downstream pressure both affect the driving force for the solids flow through the lift tube: the immersion depth should be maximized and the downstream pressure minimized in order to maximize the solids flowrate. Since the immersion depth is affected by the fluidization velocity, increasing the fluidization velocity increases the solids flow.

Experiments with various motive gases showed that although a low molecular weight motive gas has a higher sonic velocity, it is unable to transport more solids per kilogram of gas. Song et al. [6] observed the same trends with a draft tube in a similar setup.

Heat transfer between fluidized beds was increased from 25 to 400 W/m²K with the implementation and optimization of a single

lift tube. The physical setup and the operating gas flowrate can be altered with this information in order to optimize the solids circulation flowrate through the lift tube. This is essential in order to minimize costs associated with high flow compressors and gas phase heat recovery equipment. While the main application for these experiments has been the Agri-Therm mobile pyrolysis reactor, it is also possible to apply this technology to other fluidized bed processes.

Acknowledgements

We would like to thank Jim Weaver, Ron Golden, Caprex Ltd and Agri-Therm for their technical and financial support. We gratefully acknowledge the contributions of the Ontario government in the form of an Ontario Graduate Scholarship to Mike Jacobson and in the form of an Ontario Centres of Excellence grant.

References

- [1] C. Wen, E. Miller, *Ind. Eng. Chem.* 53 (1) (1961) 51–53.
- [2] R. Wu, J. Grace, C. Lim, C. Brereton, *AIChE J.* 35 (10) (1989) 1685–1691.
- [3] Dz. Hadzinmajlovic, Z. Grbavcic, S. Povrenovic, D. Vukovic, R. Garvic, *Fluidization VII: Proceedings of the Seventh Engineering Foundation Conference on Fluidization*, New York, USA, May 3–8, 1992, pp. 337–344.
- [4] J.-Y. Zhang, H. Pen, B.-X. Li, J.-F. Wang, Y.-A. Cao, *Circulating Fluidized Bed Technology V*, Science Press, Beijing, 1996, pp. 388–393.
- [5] W. Lee, S. Kim, *Fluidization VII: Proceedings of the Seventh Engineering Foundation Conference on Fluidization*, New York, USA, May 3–8, 1992, pp. 479–486.
- [6] B. Song, Y. Kim, S. Kim, *Chem. Eng. J.* 68 (1997) 115–122.
- [7] W. Yang, D. Keairns, *Can. J. Chem. Eng.* 61 (1983) 349–363.
- [8] J. Muir, F. Berruti, L. Behie, *Chem. Eng. Commun.* 88 (1990) 153–171.
- [9] C. Hulet, C. Briens, F. Berruti, E. Chan, *Powder Technol.* 185 (2) (2008) 131–143.
- [10] C. Hulet, C. Briens, F. Berruti, E. Chan, *Chem. Eng. Process* 47 (9–10) (2008) 1435–1450.
- [11] F. Zenz, D. Othmer, *Fluidization and Fluid-Particulate Systems*, Reinhold, New York, NY, 1960, pp. 318–319.